Available online at www.sciencedirect.com
SCIENCE DIRECT
Journal of Molecular Catalysis A: Chemical 246 (2006) 1–10
JOURNAL OF MOLECULAR CATALYSIS A: CHEMICAL
www.elsevier.com/locate/molcata

A computational study of methane catalytic reactions on zeolites

Xiaobo Zheng, Paul Blowers *

Department of Chemical and Environmental Engineering, The University of Arizona, PO Box 210011, Tucson, AZ 85721-0011, USA

Received 25 August 2005; received in revised form 9 October 2005; accepted 10 October 2005
Available online 18 November 2005

Abstract

The cluster approach method is used to study the transition state structures and the activation barriers of methane hydrogen exchange and dehydrogenation reactions catalyzed by zeolites. The reactant and transition state structures are optimized at the B3LYP/6-31g* level, and the energies are calculated using CBS-QB3, a complete basis set composite energy method. The computed activation barriers are 33.53 kcal/mol for the hydrogen exchange reaction and 90.08 kcal/mol for the dehydrogenation reaction. The effects of zeolite acidity on the reaction barriers are also investigated by changing the length of the terminal Si–H bonds. Analytical expressions between activation barriers and zeolite deprotonation energies for each reaction are proposed so accurate activation barriers can be obtained when using different zeolites as catalysts. Additionally, transition state theory is applied to estimate the reaction rate constants of the hydrogen exchange and dehydrogenation reactions from calculated activation barriers, and vibrational, rotational and translational partition functions.

Keywords: Methane; Zeolite; Cluster approach; CBS method

1. Introduction

Hydrocarbon conversion processes are essential for the modern oil and chemical industries [1,2]. In these processes, zeolites are extensively used as catalysts and the world-wide total annual consumption reached 360 million tons in 1998 [3]. Zeolites have lattice structures and the Brønsted site is established by replacing the lattice silicon atom, which has a formal valency of four, with an aluminum atom that has a valency of three. A proton is attached to the oxygen atom connecting the silicon to its aluminum atom neighbor, resulting in a chemically stable structure where the oxygen atom becomes a three-coordinated structure. The highly acidic proton attached to the oxygen atom makes a zeolite a good catalyst [4].

Catalytic conversion of methane to liquid fuels or desired products is currently one of the great challenges in catalysis science [5]. Also, methane catalytic conversion reactions are among the simplest elementary reactions, which can be studied experimentally. By comparing theoretical results with the experimental data, these reactions can be used as benchmarks to evaluate the accuracy of computational methods.

In applying computational chemistry to study a catalytic reaction system, the first step is to choose a structural model to represent the catalyst. The zeolite cluster model, $H_3Si–O–AlH_2–(OH)–SiH_3$, is a typical one used to model the Brønsted acid site of a zeolite catalyst [6,7]. This model is referred as a T3 cluster, denoting the presence of three tetrahedral atoms (one aluminum and two silicon). In previous work, the calculated geometry and frequency results of this cluster model were compared with available experimental data [8–12] and showed excellent agreement for the acidic hydrogen and aluminum atom distance and the acidic H–O bond vibrational frequency [13]. Furthermore, this cluster model has a deprotonation energy close to those found for high-silica acidic zeolites, around 295.4 kcal/mol [6,14–16]. Also, it has proven to be large enough to include the important neighborhood surrounding the Brønsted acid site, but is still small enough to allow for the application of high-level quantum chemical treatment [7,17]. Therefore, the T3 cluster will be the primary cluster used in this work.

For many years, researchers have used quantum chemical tools to investigate the structure, stability, reaction kinetics, and mechanisms of different molecular systems [18–27] particularly, density functional theory and ab initio methods have been applied by to study catalytic reactions quantitatively [13,28–40]. Kramer et al. studied the methane hydrogen exchange reaction

* Corresponding author. Tel.: +1 520 626 5319; fax: +1 520 621 6048.
E-mail address: blowers@engr.arizona.edu (P. Blowers).

1381-1169/$ – see front matter © 2005 Elsevier B.V. All rights reserved.
doi:10.1016/j.molcata.2005.10.009

using HF/6-31g** calculations, a low level ab initio method with a modest basis set [41]. Evleth et al. investigated the methane hydrogen exchange reaction using MP2/6-31++g*//HF/3-21g (energy calculation method//geometry optimization method) with a silicon-free T1 cluster [42]. The activation barriers obtained are relatively high in that work, reflecting the inability of a T1 cluster to represent a zeolite catalyst. In 1999, Esteves et al. studied the methane hydrogen exchange reaction using B3LYP/6-31g** and MP2/6-31g**//HF/6-31g** methods [17]. The activation barriers for the methane hydrogen exchange reaction were 32.3 and 31.1 kcal/mol using these methods. In 2000, Ryder et al. studied the methane hydrogen exchange reaction using the BH&HLYP/6-31++g** method [43]. The activation barrier obtained with this method was 38.4 kcal/mol. Kazansky et al. also investigated methane hydrogen exchange and dehydrogenation reactions using a small T1 cluster and the low level HF/3-21g method [44]. The activation barriers obtained were 37.1 kcal/mol for hydrogen exchange and 104.5 kcal/mol for dehydrogenation. With a T3 cluster model, Blaszkowski et al., studied the methane reaction using BP/DZPV, a nonlocal density functional theory method [45]. The resulting activation barriers were relatively low, 29.85 kcal/mol for hydrogen exchange and 82.03 kcal/mol for dehydrogenation because the BP/DZPV method tends to underestimate reaction barriers for this type of reaction [46]. Finally, to complete the short list of previous work on this topic, Larson et al., experimentally investigated the CD_4 H/D reaction using silica-alumina catalysts and reported an activation energy of 33.4 kcal/mol [47].

In this work, a silicon-containing T3 cluster is used to simulate the zeolite catalyst, and a high level composite energy method is implemented to investigate the methane hydrogen exchange and dehydrogenation reaction energetics. The results are then compared with the experimental data and computational results from other researchers. Furthermore, the influence of the zeolite acidity on methane conversion reaction activation barriers is studied quantitatively. Calculations of the reaction rate constants using canonical transition state theory are also reported.

2. Computational methods

Density functional theory (DFT) has been widely applied by physicists to study the electronic structure of solids in the past 30 years [19–21,28,32,48–55]. Computational studies of chemical reaction systems have become very popular because the methods are quite reliable and only have medium computational demands compared to ab initio molecular orbital theory. The geometry optimizations of the reactants, products, and transition state structures in this work were carried out using Becke's three-parameter density functional [56] and the Lee, Yang, and Parr functional [57] to describe gradient-corrected correlation effects, which leads to the well-known B3LYP method, combined with a moderate basis set, 6-31g*. The B3LYP method has been validated to give results similar to that of the more computationally expensive MP2 theory for molecular geometry and frequency calculations [58,59].

It has been pointed out by many researchers that the calculated activation barriers strongly depend on the level of the final energy calculations and less on the level of the geometry optimisation [32,60,61]. Therefore, it is advisable to perform the geometry optimizations at a relatively lower level, B3LYP/6-31g* in this work, and the final energy calculations at a higher level, CBS-QB3, a complete basis set composite energy method. Traditionally, energy calculations contain only a single computation. To obtain accurate energies, one generally requires a large basis set with a high level method, which generally takes significant time to compute. Composite energy methods are composed of a series of single point energy calculations steps. Their results are then combined to obtain the highly accurate energy value at a reduced computational cost. The recently developed complete basis set (CBS) methods [62–70] include the basis set truncation errors, the major defect encountered for the single point energy calculations. In 1999, Montgomery et al. proposed a complete basis set method using density functional geometry and frequencies, referred to as the CBS-QB3 method [65]. For the G2 test set of first-row molecules, the mean absolute error for a wide variety of highly accurate experimental energies is decreased to 0.87 kcal/mol for the CBS-QB3 method compared to 1.37 kcal/mol for the G2 method [71]. In this work, the B3LYP/6-31g* method was used to calculate geometries and frequencies in the CBS-QB3 formalism.

The geometry optimizations are performed with the GAUSSIAN98 [72] software package. All the structures were fully optimized without geometry constraints. The products and reactants were verified with frequency calculations to be stable structures, and the transition states were tested to ensure they were first order saddle points with only one negative eigenvalue. Additionally, intrinsic reaction coordinate (IRC) calculations proved that each reaction linked the correct products with reactants. Zero point vibrational energies (ZPVE) were obtained from harmonic vibrational frequencies calculated at the B3LYP/6-31g* level with a scaling factor of 0.9806 and the frequencies were scaled by 0.9945 [73]. These frequencies were used in the partition functions for the prediction of reaction rates using transition state theory [74–77]. Also, thermal corrections were included in addition to the ZPVE at all temperatures where reaction rate constants were calculated.

3. Results and discussions

3.1. Hydrogen exchange reaction

$$CH_4 + H_3SiOAlH_2(OH')SiH_3 \rightarrow CH_3H' + H_3Si(OH)AlH_2OSiH_3$$

The hydrogen exchange reaction consists of the cleavage of one methane C–H bond and the formation of another C–H′ bond to the zeolite acidic proton. Fig. 1(a) shows the calculated transition state structure for the hydrogen exchange reaction of methane using the B3LYP/6-31g* method. The structure clearly shows the C_s symmetry obtained without any symmetry constraints applied for the optimization calculation. The protonated

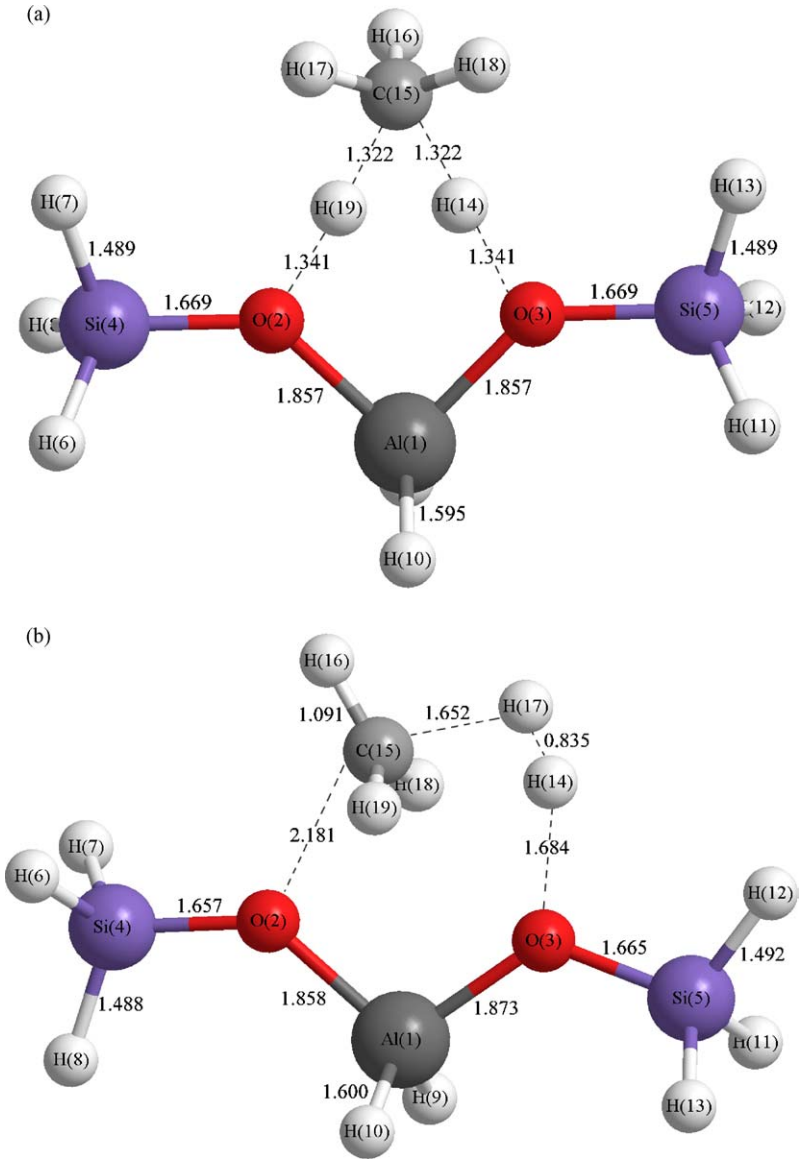

Fig. 1. Transition state structures for methane reactions on a T3 zeolite cluster optimized at the B3LYP/6-31g* level for (a) hydrogen exchange reaction, (b) dehydrogenation reaction (units in Å).

carbon, C (15), stays in the main plane of zeolite cluster and becomes a penta-coordinated structure. The acidic proton H(14) and the hydrogen atom from the methane molecule H(19) stay in the middle of the carbon and oxygen atoms, indicating formation of one C–H bond and breaking of the other. In the reaction process, the right oxygen of the cluster acts as a Brønsted acid which donates a proton while the left oxygen acts as a Lewis base which receives the hydrogen atom from methane.

The activation barrier calculated using the CBS-QB3 composite energy method is 33.53 kcal/mol. As listed in Table 1,

Table 1
Activation barrier results from theory and experiment for methane reactions on zeolites (units in kcal/mol)

	This work	Kramer [41]	Evleth, 1994 [42]	Esteves, 1999 [17]	Ryder [43]	Kazansky [44]	Blaszkowski [45]	Experiment [47]
Cluster Model/ Catalyst Type	T3	T3	T1	T3	T5	T1	T3	H-ZSM-5
Geometry Opt.	B3LYP/6-31g*	HF/6-31g**	HF/6-31g*	B3LYP/6-31g**	BH&HLYP/6-31++g**	HF/3-21g	BP/DZVP	
Energy Calculation	CBS-QB3	HF/6-31g**	MP2/6-31++g*	B3LYP/6-31g**	BH&HLYP/6-31++g**	HF/3-21g	BP/DZVP	
Hydrogen Exchange	33.53	35.90	39.90	32.30	38.40	37.10	29.85	33.40
Dehydrogenation	90.08	–	–	–	–	104.50	82.03	–

the result is compared with experimental data and computational results from other researchers. An experimental study from Larson et al., determined the activation barrier for deuterium exchange reaction of CD_4 with zeolite type H-ZSM-5 to be 33.4 kcal/mol. The difference between our calculated result with the experimental value is only 0.13 kcal/mol, which shows our choice of zeolite cluster model and computational method can reproduce experiment very well. In 1993, Kramer et al., studied the methane hydrogen exchange reaction using HF/6-31g** calculations and a T3 cluster. The activation barrier obtained, 35.90 kcal/mol, is higher than the experiment. The reason is that the HF energy calculations tend to overestimate barrier heights [78–81]. In 1994, Evleth et al., performed a similar calculation using MP2/6-31++g*//HF/3-21g method and a silicon-free T1 cluster [42]. The activation barrier obtained, 39.90 kcal/mol, is relatively high, reflecting that the T1 cluster cannot represent the zeolite catalyst properly because it does not contain important characteristics of a real zeolite, the Si–O–Al bridge [82]. In 1999, Evleth et al., extended their early work using B3LYP/6-31g** and MP2/6-31g**//HF/6-31g** methods with the T3 cluster model [17]. The activation barriers for the methane hydrogen exchange reaction were 32.3 kcal/mol and 31.1 kcal/mol, respectively. Kazansky et al., investigated the methane hydrogen exchange reaction using a small T1 cluster and the low level HF/3-21g method [44]. The activation barriers obtained was 37.1 kcal/mol, again overestimating the barrier like HF methods often do. With a T3 cluster model, Blaszkowski et al., studied the methane reaction using BP/DZPV, a nonlocal density functional theory method. The resulting activation barriers are relatively low, 29.85 kcal/mol, because the BP/DZPV method tends to underestimate reaction barriers in this type of reactions [46]. Recently, Ryder et al., studied the methane hydrogen exchange reaction using the BH&HLYP/6-31++g** method and a large T5 cluster model [43]. The activation barrier result was 38.4 kcal/mol, which is still higher than the experimental value. Compared with the more accurate result of this work using a relatively smaller T3 cluster model, this highlights the importance of the energy calculation method. Without further increasing the zeolite cluster size, accurate results can be obtained as long as the energy is obtained at a high level, CBS-QB3 in this work.

3.2. Dehydrogenation reaction

$$CH_4 + H_3SiOAlH_2(OH)SiH_3 \rightarrow H_2 + H_3Si(OCH_3)AlH_2OSiH_3$$

The dehydrogenation reaction consists of cleavage of a C–H bond by the zeolite Brønsted acid proton. The fully optimized transition state structure of the reaction is shown in Fig. 1(b). The H(16)-C(15)–H(18)–H(19) structure becomes planar. A six member ring, O(2)–Al(1)–O(3)–H(14)–H(17)–C(15), is formed. With the H(17)–C(15) and H(14)–O(3) distances greatly extended, a di-hydrogen molecule is almost formed, whereas the CH_3 group binds to the zeolite oxygen, O(2). In this reaction, the right oxygen O(3) acts as a Brønsted acid which donates a proton and the left oxygen O(2) acts as a Lewis base which receives the CH_3 group.

The activation barrier obtained using the CBS-QB3 method is 90.08 kcal/mol. This barrier is much higher than the hydrogen exchange reaction activation barrier, indicating the reaction is more difficult to take place. Unfortunately, direct comparison to experiment cannot be made because there are no experimental activation energies available for this reaction. Instead, the result obtained in this work is compared with the computational results from other researchers. Blaszkowski et al., studied this reaction using BP/DZPV, a nonlocal density functional theory method and a T3 cluster. The resulting activation barrier, 82.03 kcal/mol, was probably low because the BP/DZPV method tends to underestimate reaction barriers for this type of reaction [46]. The activation barrier obtained Kazansky et al., using HF/3-21g and a T1 cluster is 104.5 kcal/mol. This is relatively higher than the result of this work because the small T1 cluster is unable to represent the zeolite catalyst and the HF method tends to overestimate activation barriers [78–81]. The comparison showed in the earlier section suggests our result is expected to be accurate although experimental measurements for this reaction are still not available.

3.3. Acidity effects

The zeolite acidity plays a very important role in studying reaction properties for the systems like those examined in this work. In this section, we investigate the effect of zeolite acidity for the methane conversion reactions. The deprotonation energy (E_{dep}) is a theoretical measurement of zeolite acidity and is defined as the energy difference between the protonated (ZH) and unprotonated (Z^-) clusters [83].

$$E_{dep} = E(Z^-) - E(ZH)$$

In real zeolite catalysts, the deprotonation energy varies over a range of 20–50 kcal/mol among different zeolite structures [15,16,83–87]. Kramer et al., [41,88] have shown that the acidity effect of zeolite catalysts can be simulated by modifying the length of the terminal Si–H bonds of the cluster model with all other geometry parameters fully optimized, and our previous work has successfully applied this methodology [13]. Fig. 2 shows the effect of the terminal Si–H distance on the zeolite cluster geometries. The geometry shown is obtained at the B3LYP/6-31g* level. The neighbor Si–O bond length decreases from 1.72 to 1.698 Å and the protonic hydrogen and acidic oxygen bond distance, H(14)–O(3) increases slightly from 0.975 to 0.979 Å as the Si–H bond length changes from 1.30 to 1.70 Å. This indicates that this O–H bond becomes weaker with the increasing distance of the Si–H bond. Therefore, the zeolite cluster becomes more acidic. Increasing the Si–H bond length on the left side of the cluster only has a slight effect on the O–H bond because the Si and protonic H atoms are so far apart.

The changes in the zeolite acidity have a corresponding affect on the transition state structures and activation barriers of the reactions. Fig. 3 shows the transition state structures of the methane hydrogen exchange reaction as the Si–H distance changes from 1.3 to 1.9 Å. With Si–H bond length

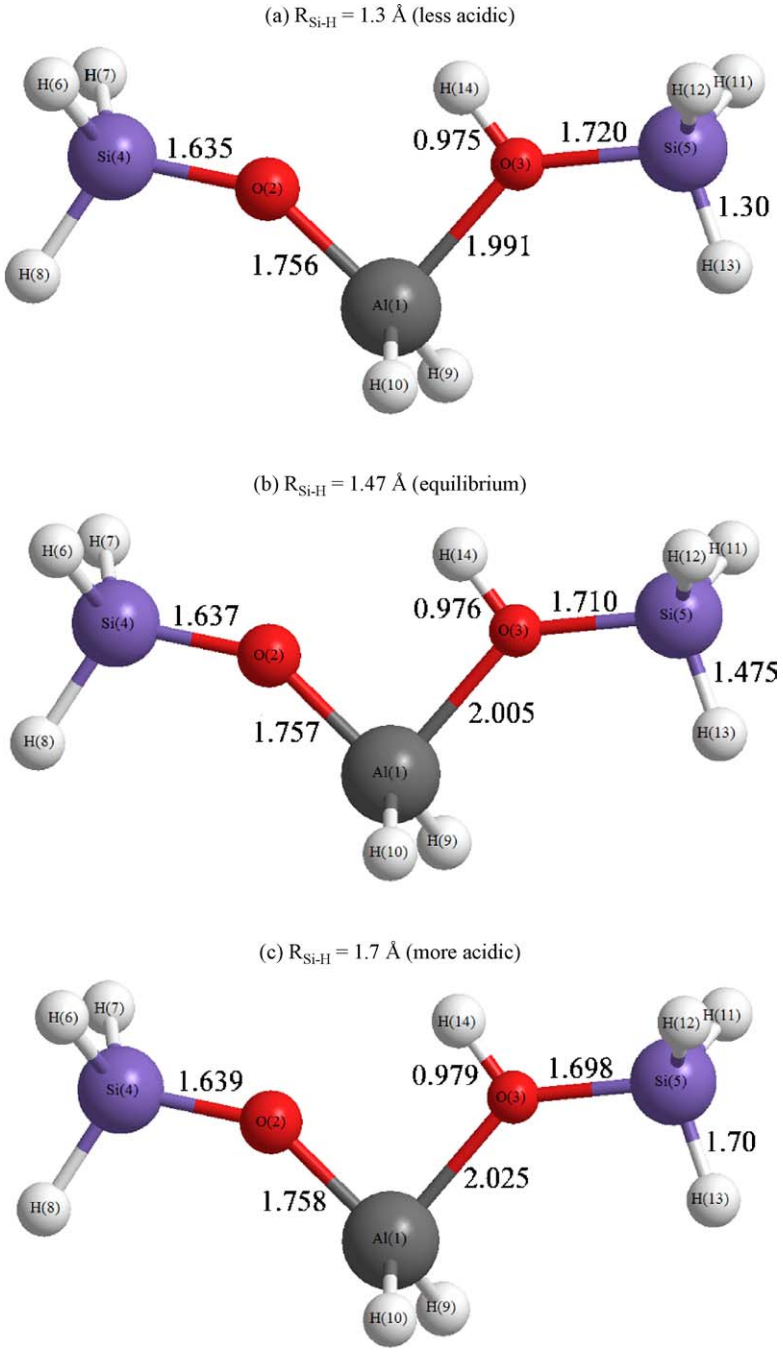

Fig. 2. $H_3Si{-}O{-}AlH_2{-}(OH){-}SiH_3$ cluster structures with changing terminal Si–H bond distances (units in Å).

increase, the distance of the protonic hydrogen and acidic oxygen, H(14)–O(3), increases from 1.329 to 1.361 Å. Similarly, the distance between the exchanging hydrogen and Lewis basic oxygen, H(19)–O(2), increases from 1.313 to 1.407 Å and the CH_5 group moves further away from the cluster. Meanwhile, the two exchanging hydrogens, H(14) and H(19), stay closer to the CH_3 group.

Similar acidic studies were applied to the methane dehydrogenation reaction as well. However, a transition state cannot be located as the Si–H distance increases to 1.9 Å due to computational difficulties. The transition state structures of the methane dehydrogenation reaction as the Si–H distance changes to 1.3 and 1.7 Å are shown in Fig. 4. As the Si–H distance increases, the distance of carbon atom and Lewis basic oxygen, C(15)–O(2), increases from 2.151 to 2.229 Å and the distance of protonic hydrogen and acidic oxygen, H(14)–O(3) increases from 1.615 to 1.811 Å. Meanwhile, the bi-hydrogen, H(14) and H(17), atoms move closer to each other from 0.849 to 0.818 Å, which is more like the structure of a hydrogen molecule, and the entire CH_5 group moves further away from the cluster.

Table 2 shows the change in activation barriers of methane conversion reactions as the zeolite cluster Si–H bond distances

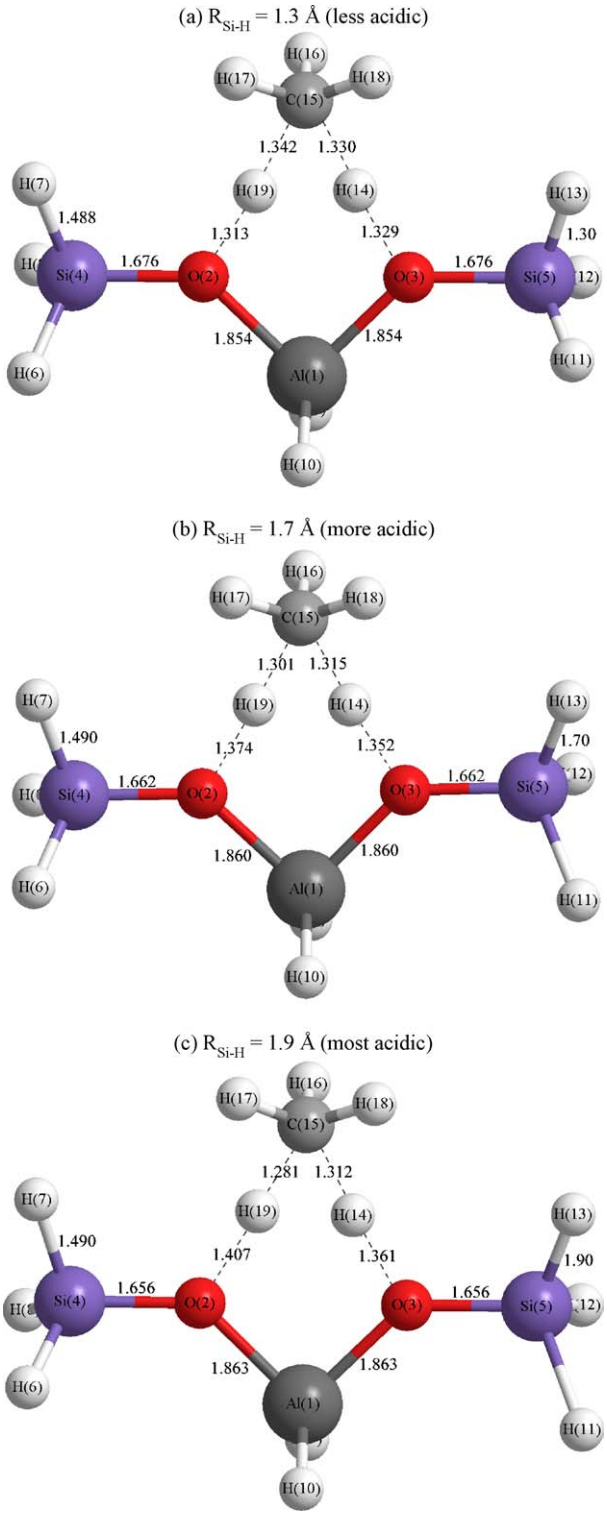

Fig. 3. Transition state structures for the methane hydrogen exchange reaction with changing terminal Si—H bond distances (units in Å).

are varied. With the Si–H distance increasing, the activation barriers decrease for the reactions because of the increased acidity of the zeolite cluster. As long as the reaction mechanism does not alter, the change in activation barrier is linearly correlated to the change in deprotonation energy. Therefore, the Brøsted-Polanyi principle can be applied [89]: $\Delta E_a = c\Delta E_{dep}$ or $\Delta E_a = c\Delta E_{dep} + b$.

The linear relationship of the activation barriers with cluster deprotonation energies is illustrated in Fig. 5. Applying the deprotonation energy of the most commonly used zeolite–H-ZSM-5, 295.40 kcal/mol [6,14–16], the activation barriers are then calculated and listed in Table 2. For the dehydrogenation reaction, the ratio of the change in activation barrier to the change in zeolite deprotonation energy is 0.6453, which is almost identical to that from previous work on ethane conversion reactions on zeolite [13], 0.6509. For hydrogen exchange, the ratio becomes 0.3523, slightly less than that of ethane, 0.403. Further work needs to verify if these ratios hold for other larger *n*-alkane reactions on zeolites.

The acidity effect study has shown the correlations between the deprotonation energies and activation barriers for methane conversion reactions. Because deprotonation energies are significantly easier to calculate than activation barriers due to the difficulty in performing transition state optimizations for large complexes with many degrees of freedom, using the correlations, activation barriers can be more easily obtained for different zeolite catalysts as long as their deprotonation energies are first acquired from theory or experiment.

3.4. Reaction rate constant estimations

Canonical transition state theory [74–77] is broadly used to predict reaction rate constants using the computational results. For methane conversion reactions, the rate constants can be expressed as:

$$k_r = \left(\frac{k_B T}{h}\right) N_A \frac{q_{TS}^{\mp}}{q_{CH_4} q_{T3}} \exp\left(-\frac{E_{act}}{k_B T}\right)$$

where h, k_B and N_A are the Boltzmann, Planck and Avogadro constants; $q_{TS}^{\mp}$, q_{CH_4} and q_{T3} are the partition functions of the transition state structure, methane reactant, and zeolite T3 cluster, which include electronic, translational, rotational, and vibrational partition functions. Since the zeolite cluster is part of a solid, translational and rotational partition functions for the zeolite are assumed to be equal in the reactant and transition state.

Table 2
Effects of Si—H distances on methane reaction activation barriers (units in kcal/mol)

	Activation barrier (E_a)		Deprotonation energy (E_{dep})
	Dehydrogenation	Hydrogen exchange	
R_{Si-H} = 1.30 Å	93.31	35.61	303.99
R_{Si-H} = 1.47 Å	90.08	33.53	297.93
R_{Si-H} = 1.70 Å	85.33	31.16	291.59
R_{Si-H} = 1.90 Å	–	29.25	285.81
H-ZSM5[a]	88.01	32.58	295.40
Relationship	$E_a = 0.6453E_{dep} - 102.61$	$E_a = 0.3525E_{dep} - 71.55$	

[a] Ref. [16].

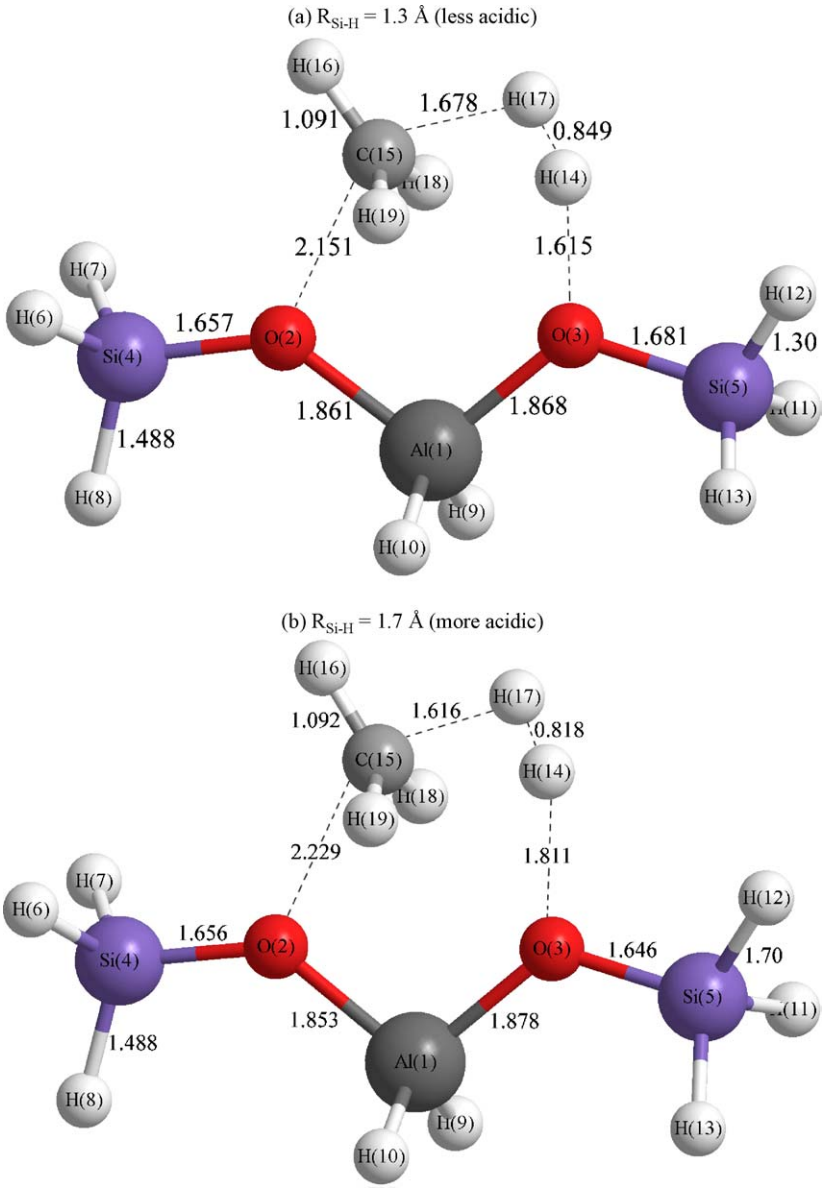

Fig. 4. Transition state structures for the methane dehydrogenation reaction with changing terminal Si—H bond distances (units in Å).

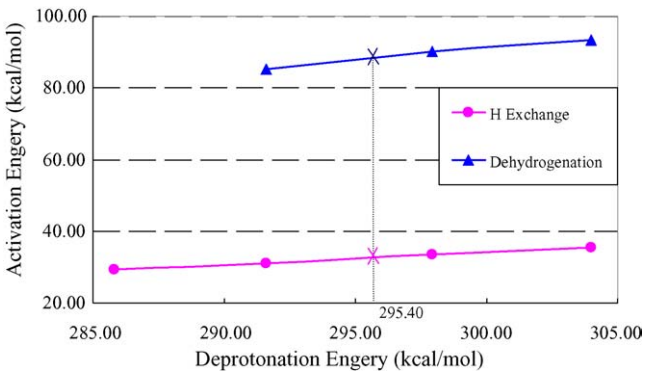

Fig. 5. Correlations of the calculated methane reactions activation barriers for the acidity effects represented by deprotonation energies.

Therefore, the rate constants are expressed as:

$$k_r = \left(\frac{k_B T}{h}\right) N_A \frac{q^{\mp}_{TS,vib}}{q_{CH_4} q_{T3,vib}} \exp\left(-\frac{E_{act}}{k_B T}\right)$$

Tunneling is a quantum effect where reactant molecules that do not have enough energy to cross the barrier can still sometimes react. Tunneling effects can be calculated with the following formula: [90]

$$\kappa(T) = 1 + \frac{1}{24}\left(\frac{h\nu c}{k_B T}\right)^2$$

where c is the speed of light; ν is the imaginary frequency that accounts for the vibrational motion along the reaction path; and, $\kappa(T)$ is the tunneling coefficient. Therefore, the reaction rate constants can be calculated as: $k = \kappa(T)k_r$.

Table 3
Rate constants of methane conversion reactions (Units in m^3/mol s for A and k; in kcal/mol for E_{act})

T	Hydrogen exchange reaction			Dehydrogenation reaction		
	A	E_{act}	k	A	E_{act}	k
300	1.15×10^5	33.99	1.92×10^{-20}	7.84×10^3	90.08	1.67×10^{-62}
400	2.42×10^5	34.58	3.00×10^{-14}	9.08×10^3	90.61	2.61×10^{-46}
500	3.32×10^5	35.30	1.20×10^{-10}	1.22×10^4	91.25	1.48×10^{-36}
800	1.06×10^6	37.93	4.54×10^{-05}	3.65×10^4	93.49	1.01×10^{-21}
1000	2.30×10^6	39.84	4.45×10^{-03}	7.33×10^4	95.02	1.22×10^{-16}
1250	5.62×10^6	42.26	2.27×10^{-01}	1.60×10^5	96.89	1.78×10^{-12}

The pre-exponential factor, $A = (k_B T/h) N_A (q^{\mp}_{TS,vib}/q_{CH_4} q_{T3,vib})$, and activation energy E_{act} of the methane hydrogen exchange reaction and dehydrogenation reactions under different temperatures are listed in Table 3. The partition functions and activation barriers were calculated separately at each temperature point. One can see that the activation barriers increase as temperature increases. This shows that it is very important to include the thermal corrections in the activation energy calculations for this system in order to obtain accurate kinetic information in the next step.

The reaction rate constant plot is shown in Fig. 6. The rate constants of hydrogen exchange reaction are much higher than those of dehydrogenation reaction because its activation barrier is much lower. A linear relationship of log(k) with respect to $1/T$ is regressed and the kinetic models are described as:

$k = 1.41 \times 10^5 \exp(-17221.96/T)$ for hydrogen exchange reaction

$k = 6.28 \times 10^3 \exp(-45409.28/T)$ for dehydrogenation reaction

The advantage of these simple models is that they can be easily applied at different temperatures where data is not available, and they have broad applications to the modern oil and chemical industries where methane conversion reaction kinetics is of concern.

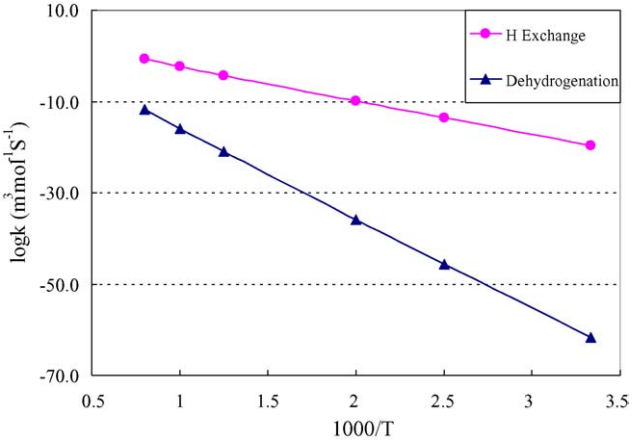

Fig. 6. Canonical transition state theory rate constants for methane reactions on a zeolite T3 cluster using B3LYP/6-31g* geometry optimizations and CBS-QB3 composite energies (Units in Kelvin for T).

4. Conclusions

In this work, methane hydrogen exchange and dehydrogenation reactions catalyzed by a zeolite were studied using a complete basis set composite energy theory and T3 cluster. The reactants, products and transition state structures were optimized using the B3LYP/6-31g* method, and the energies were obtained using the CBS-QB3 composite energy method.

The activation barriers obtained for hydrogen exchange and dehydrogenation reactions are 33.53 and 90.08 kcal/mol, respectively. This indicates that the hydrogen exchange reaction has a lower barrier and is the faster reaction to happen, while the dehydrogenation reaction has the higher barrier and has a slower rate. This may also be why the dehydrogenation reaction has been so difficult to identify experimentally since other reaction pathways will dominate at the temperatures where the experiments are typically done.

Also, the zeolite acidity effect was mimicked by changing the terminating Si–H bond lengths. Relationships between the activation barriers and deprotonation energies were proposed so that reaction barriers could be obtained when using zeolite catalysts with different acidities. Additionally, canonical transition state theory was applied to obtain reaction rate constants from the activation barriers and partition functions. The need for high quality energies was highlighted in the context of including thermal corrections to activation barriers.

Acknowledgements

This work was funded by the State of Arizona through the Office of the Vice President for Research at the University of Arizona. Supercomputer time was provided by the National Computational Science Alliance and used the NCSA HP/Convex Exemplar SPP-2000 at the University of Illinois at Urbana-Champaign. Part of the supercomputer time was provided by National Partnership for Advanced Computational Infrastructure and used the IBM pSeries 690 and pSeries 655 at Boston University.

References

[1] B.W. Wojciechowski, A. Corma, Catalytic Cracking: Catalysts, Chemistry and Kinetics, Dekker, New York, 1986.
[2] I.E. Maxwell, W.H.J. Stork, Stud. Surf. Sci. Catal. 137 (2001) 747 (Introduction to Zeolite Science and Practice (2nd ed.)).

[3] T. Maesen, B. Marcus, Stud. Surf. Sci. Catal. 137 (2001) 1 (Introduction to Zeolite Science and Practice (2nd ed.)).
[4] E.M. Flanigen, Stud. Surf. Sci. Catal. 137 (2001) 11 (Introduction to Zeolite Science and Practice (2nd ed.)).
[5] J.M. Vollmer, T.N. Truong, J. Phys. Chem. B 104 (2000) 6308.
[6] M.V. Frash, R.A. van Santen, Top. Catal. 9 (1999) 191.
[7] L.A. Curtiss, M.S. Gordon, Computational materials chemistry methods and applications, Kluwer Academic Publishers, Dordrecht, Boston, London, 2004.
[8] D. Freude, J. Klinowski, H. Hamdan, Chem. Phys. Lett. 149 (1988) 355.
[9] N.P. Kenaston, A.T. Bell, J.A. Reimer, J. Phys. Chem. 98 (1994) 894.
[10] M.A. Makarova, A.F. Ojo, K. Karim, M. Hunger, J. Dwyer, J. Phys. Chem. 98 (1994) 3619.
[11] L.M. Kustov, V.B. Kazansky, S. Beran, L. Kubelkova, P. Jiru, J. Phys. Chem. 91 (1987) 5247.
[12] M. Trombetta, T. Armaroli, A.G. Alejandre, J.R. Solis, G. Busca, Appl. Catal. A: Gen. 192 (2000) 125.
[13] X. Zheng, P. Blowers, J. Mol. Catal. A 229 (2005) 77.
[14] R.A. van Santen, B. van de Graaf, B. Smit, Studies in Surface Science and Catalysis 137 (2001) 419 (Introduction to Zeolite Science and Practice (2nd ed.)).
[15] J. Sauer, M. Sierka, J. Comput. Chem. 21 (2000) 1470.
[16] K. Sillar, P. Burk, J. Mol. Struct. Theochem. 589 (2002) 281.
[17] P.M. Esteves, M.A.C. Nascimento, C.J.A. Mota, J. Phys. Chem. B 103 (1999) 10417.
[18] B.J. Lynch, D.G. Truhlar, J. Phys. Chem. A 105 (2001) 2936.
[19] B.S. Jursic, J Chem. Soc. Perkin Trans. 2 (1997) 637.
[20] T.N. Truong, T.T.T. Truong, Chem. Phys. Lett. 314 (1999) 529.
[21] T.N. Truong, J. Chem. Phys. 113 (2000) 4957.
[22] P. Blowers, R. Masel, AIChE J. 46 (2000) 2041.
[23] M.W. Wong, L. Radom, J. Phys. Chem. A 102 (1998) 2237.
[24] M.W. Wong, L. Radom, J. Phys. Chem. 99 (1995) 8582.
[25] M.W. Wong, A. Pross, L. Radom, J. Am. Chem. Soc. 116 (1994) 6284.
[26] Y.T. Xiao, J.M. Longo, G.B. Hieshima, R.J. Hill, Ind. Eng. Chem. Res. 36 (1997) 4033.
[27] M. Saeys, M.F. Reyniers, G.B. Marin, J. Phys. Chem. A 107 (2003) 9147.
[28] P.J. Hay, A. Redondo, Y.J. Guo, Catal. Today 50 (1999) 517.
[29] S.A. Zygmunt, L.A. Curtiss, P. Zapol, L.E. Iton, J. Phys. Chem. B 104 (2000) 1944.
[30] A.M. Rigby, G.J. Kramer, R.A. van Santen, J. Catal. 170 (1997) 1.
[31] S.J. Collins, P.J. Omalley, J. Catal. 153 (1995) 94.
[32] M.V. Frash, V.B. Kazansky, A.M. Rigby, R.A. van Santen, J. Phys. Chem. B 102 (1998) 2232.
[33] J. Abbot, P.R. Dunstan, Ind. Eng. Chem. Res. 36 (1997) 76.
[34] V.B. Kazansky, M.V. Frash, R.A. van Santen, Appl. Catal. A: Gen. 146 (1996) 225.
[35] V.B. Kazansky, Catal. Today 51 (1999) 419.
[36] V.B. Kazansky, M.V. Frash, R.A. van Santen. in: 11th International Congress on Catalysis-40th Anniversary, vol. 101, 1996, p 1233 (Studies in Surface Science and Catalysis).
[37] S.J. Collins, P.J. Omalley, Chem. Phys. Lett. 228 (1994) 246.
[38] P. Viruelamartin, C.M. Zicovichwilson, A. Corma, J. Phys. Chem. 97 (1993) 13713.
[39] V.B. Kazansky, I.N. Senchenya, M. Frash, R.A. van Santen, Catal. Lett. 27 (1994) 345.
[40] V.B. Kazansky, M.V. Frash, R.A. van Santen, Catal. Lett. 28 (1994) 211.
[41] G.J. Kramer, R.A. van Santen, C.A. Emeis, A.K. Nowak, Nature 363 (1993) 529.
[42] E.M. Evleth, E. Kassab, L.R. Sierra, J. Phys. Chem. 98 (1994) 1421.
[43] J.A. Ryder, A.K. Chakraborty, A.T. Bell, J. Phys. Chem. B 104 (2000) 6998.
[44] V.B. Kazansky, M.V. Frash, R.A. van Santen, Catal. Lett. 28 (1994) 211.
[45] S.R. Blaszkowski, A.P.J. Jansen, M.A.C. Nascimento, R.A. van Santen, J. Phys. Chem. 98 (1994) 12938.
[46] Q. Zhang, R. Bell, T.N. Truong, J. Phys. Chem. 99 (1995) 592.
[47] J.G. Larson, W.K. Hall, J. Phys. Chem. 69 (1965) 3080.
[48] A. Bottoni, J. Chem. Soc. Perkin Trans. 2 (1996) 2041.
[49] J. Lins, M.A.C. Nascimento, J. Mol. Struc. Theochem. 371 (1996) 237.
[50] J.B. Nicholas, Top. Catal. 4 (1997) 157.
[51] E. Broclawik, H. Himei, M. Yamadaya, M. Kubo, A. Miyamoto, R. Vetrivel, J. Chem. Phys. 103 (1995) 2102.
[52] S.R. Blaszkowski, R.A. van Santen, J. Phys. Chem. 99 (1995) 11728.
[53] A. Bhan, Y.V. Joshi, W.N. Delgass, K.T. Thomson, J. Phys. Chem. B 107 (2003) 10476.
[54] N.O. Gonzales, A.K. Chakraborty, A.T. Bell, Catal. Lett. 50 (1998) 135.
[55] X. Rozanska, R.A. van Santen, T. Demuth, F. Hutschka, J. Hafner, J. Phys. Chem. B 107 (2003) 1309.
[56] A.D. Becke, J. Chem. Phys. 98 (1993) 5648.
[57] C.T. Lee, W.T. Yang, R.G. Parr, Phys. Rev. B 37 (1988) 785.
[58] B.G. Johnson, P.M.W. Gill, J.A. Pople, J. Chem. Phys. 98 (1993) 5612.
[59] C.W. Bauschlicher, H. Partridge, J. Chem. Phys. 103 (1995) 1788.
[60] M.V. Frash, V.B. Kazansky, A.M. Rigby, R.A. van Santen, J. Phys. Chem. B 101 (1997) 5346.
[61] V.B. Kazansky, M.V. Frash, R.A. van Santen, Catal. Lett. 48 (1997) 61.
[62] G.A. Petersson, A. Bennett, T.G. Tensfeldt, M.A. Allaham, W.A. Shirley, J. Mantzaris, J. Chem. Phys. 89 (1988) 2193.
[63] J.A. Montgomery, M.J. Frisch, J.W. Ochterski, G.A. Petersson, J. Chem. Phys. 112 (2000) 6532.
[64] T. Morihovitis, C.H. Schiesser, M.A. Skidmore, J. Chem. Soc. Perkin Trans. 2 (1999) 2041.
[65] J.A. Montgomery, M.J. Frisch, J.W. Ochterski, G.A. Petersson, J. Chem. Phys. 110 (1999) 2822.
[66] P.M. Mayer, C.J. Parkinson, D.M. Smith, L. Radom, J. Chem. Phys. 108 (1998) 604.
[67] J.W. Ochterski, G.A. Petersson, J.A. Montgomery, J. Chem. Phys. 104 (1996) 2598.
[68] J.A. Montgomery, J.W. Ochterski, G.A. Petersson, J. Chem. Phys. 101 (1994) 5900.
[69] G.A. Petersson, M.A. Allaham, J. Chem. Phys. 94 (1991) 6081.
[70] G.A. Petersson, T.G. Tensfeldt, J.A. Montgomery, J. Chem. Phys. 94 (1991) 6091.
[71] L.A. Curtiss, K. Raghavachari, G.W. Trucks, J.A. Pople, J. Chem. Phys. 94 (1991) 7221.
[72] M.J. Frisch, G.W. Trucks, H.B. Schlegel, P.M.W. Gill, B.G. Johnson, M.A. Robb, J.R. Cheeseman, T. Keith, G.A. Petersson, J.A. Montegomery, K. Raghavachari, M.A. Al-Laham, V.G. Zakrzewski, J.V. Ortiz, J.B. Foresman, J. Cioslowski, B.B. Stefanov, A. Nanayakkara, M. Challacombe, C.Y. Peng, P.Y. Ayala, W. Chen, M.W. Wong, J.L. Andres, E.S. Replogle, R. Gomperts, R.L. Martin, D.J. Fox, J.S. Binkley, D.J. Defrees, J. Baker, J.P. Stewart, M. Head-Gordon, C. Gonzalez, J.A. Pople Gaussian, Inc., Pittsburgh, PA, 1995.
[73] A.P. Scott, L. Radom, J. Phys. Chem. 100 (1996) 16502.
[74] R.I. Masel, Principles of Adsorption and Reaction on Solid Surfaces, Wiley, New York, 1996.
[75] R.I. Masel, Chemical Kinetics and Catalysis, Wiley-Interscience, New York, 2001.
[76] K.A. Holbrook, M.J. Pilling, S.H. Robertson, Unimolecular Reactions, John Wiley & Sons, Chichester, New York, 1996.
[77] R.G. Gilbert, S.C. Smith, Theory of Unimolecular and Recombination Reactions, Blackwell Scientific Publications, Oxford, England, 1990.
[78] B.G. Willis, K.F. Jensen, J. Phys. Chem. A 102 (1998) 2613.
[79] W.T. Lee, R.I. Masel, J. Phys. Chem. 100 (1996) 10945.
[80] W.T. Lee, R.I. Masel, J. Phys. Chem. 99 (1995) 9363.
[81] H. Yamataka, S. Nagase, T. Ando, T. Hanafusa, J. Am. Chem. Soc. 108 (1986) 601.
[82] I. Milas, M.A.C. Nascimento, Chem. Phys. Lett. 338 (2001) 67.
[83] H.V. Brand, L.A. Curtiss, L.E. Iton, J. Phys. Chem. 97 (1993) 12773.
[84] J. Datka, M. Boczar, P. Rymarowicz, J. Catal. 114 (1988) 368.

[85] U. Eichler, M. Brandle, J. Sauer, J. Phys. Chem. B 101 (1997) 10035.
[86] R. Grau-Crespo, A.G. Peralta, A.R. Ruiz-Salvador, A. Gomez, R. Lopez-Cordero, Phys. Chem. Chem. Phys. 2 (2000) 5716.
[87] K. Sillar, P. Burk, J. Phys. Chem. B 108 (2004) 9893.
[88] G.J. Kramer, R.A. van Santen, J. Am. Chem. Soc. 115 (1993) 2887.
[89] R.A. van Santen, G.J. Kramer, Chem. Rev. 95 (1995) 637.
[90] W.T. Duncan, R.L. Bell, T.N. Truong, J. Comput. Chem. 19 (1998) 1039.